

Room Temperature Instability of  $E'_{\gamma}$  Centers Induced by  $\gamma$  Irradiation in Amorphous  $\text{SiO}_2$ F. Messina,<sup>\*,†</sup> S. Agnello,<sup>†</sup> M. Cannas,<sup>†</sup> and A. Parlato<sup>‡</sup>*Dipartimento di Scienze Fisiche ed Astronomiche, Università di Palermo, Via Archirafi 36, and Dipartimento di Ingegneria Nucleare, Università di Palermo, Viale delle Scienze, Building 6, 90128 Palermo, Italy**Received: June 21, 2008; Revised Manuscript Received: November 15, 2008*

We study by optical absorption measurements the stability of  $E'_{\gamma}$  centers induced in amorphous silica at room temperature by  $\gamma$  irradiation up to 79 kGy. A significant portion of the defects spontaneously decay after the end of irradiation, thus allowing the partial recovery of the transparency loss initially induced by irradiation. The decay kinetics observed after  $\gamma$  irradiation with a 0.6 kGy dose closely resembles that measured after exposure to 2000 pulses of pulsed ultraviolet (4.7 eV) laser light of 40 mJ/cm<sup>2</sup> energy density per pulse. In this regime, annealing is ascribed to the reaction of the induced  $E'_{\gamma}$  centers with diffusing  $\text{H}_2$  of radiolytic origin. At higher  $\gamma$  doses, the decay kinetics becomes unexpectedly slower notwithstanding the progressive growth of the concentration of induced defects. In particular, the annealing kinetics of  $E'_{\gamma}$  centers after 79 kGy irradiation is inconsistent with the reaction parameters between the defect and  $\text{H}_2$ . To explain this result, on the basis of the quantitative analysis of the kinetics, we propose water-related species to be responsible for the slow room temperature annealing of  $E'_{\gamma}$  after irradiation with such a dose. This model is qualitatively supported by results obtained by IR absorption measurements, which show an increase of the absorption in the spectral region of Si–OH groups.

**Introduction**

Amorphous silicon dioxide ( $\text{a-SiO}_2$ ), or silica glass, is one of the most used materials in current optical and electronic technologies, which exploit its high optical transparency from infrared (IR) to ultraviolet (UV), its insulating nature, and its excellent workability and resistance to fabricate lenses, optical fibers, and insulating layers in metal oxide semiconductor (MOS) devices.<sup>1,2</sup> When silica-based devices are used in radioactive environments, or are subjected to high-power laser light, the exposure to radiation leads to the formation of point defects which compromise the performance of the glass, mainly due to their wide optical absorption bands.<sup>1,2</sup> One of the most important and common defects in the tetrahedral  $\text{SiO}_2$  matrix is the  $E'_{\gamma}$  center, whose fundamental moiety is a Si dangling bond ( $\equiv\text{Si}^{\bullet}$ ). The paramagnetic  $E'_{\gamma}$  center is easily induced in silica by any kind of irradiation, and its absorption band peaked at 5.8 eV constitutes one of the main causes of transparency loss of the glass in the UV range upon irradiation.<sup>1</sup>

It has been known for some time that several species such as hydrogen,<sup>3–16</sup> oxygen,<sup>17–20</sup> or water<sup>12,19,21</sup> are able to diffuse in the glass and chemically react with defects induced by irradiation, leading to their annealing.<sup>3–7,10,13–17,19–28</sup> These mechanisms allow for a partial recovery of the damage initially induced by irradiation. In most experiments, the annealing of defects is purposely induced (and studied) by subjecting the irradiated specimen to a thermal treatment. However, a few works have demonstrated that the decay of defect-related optical absorption bands can also occur spontaneously in the postirradiation stage without any need of heating the sample.<sup>13–15,22,24–27,29</sup>

Room temperature decay effects have been studied mainly for defects absorbing in the visible spectral range in optical fibers<sup>22,25–27</sup> or for defects induced in bulk silica by laser

irradiation.<sup>14,15,24</sup> In contrast, much less is known on the postirradiation stability of defects induced in bulk  $\text{SiO}_2$  by  $\gamma$  irradiation.<sup>30</sup> As a consequence, most of the existing data on the generation of point defects in  $\text{SiO}_2$  are currently based on stationary measurements, i.e., measurements carried out when the postirradiation annealing processes are concluded. Hence, the influence of diffusion/reaction processes on radiation-induced damage has been neglected, and their consequences have possibly been underestimated.

In particular, while it is known that the  $E'_{\gamma}$  center may undergo an almost complete decay when it is generated by laser radiation,<sup>14</sup> the defect is widely considered stable at room temperature on a year time scale, with a few exceptions,<sup>21</sup> when induced by ionizing radiation. Hence, it is important to elucidate under which conditions the spontaneous annealing effects occur, which chemical species are responsible for them, and to what extent they condition the concentration of induced defects. These questions remain unanswered at the moment, their experimental investigation being mandatory to extensively understand the basic radiation–matter interactions which result in the formation of defects. Finally, a few experiments have pointed out that the chemical kinetics of the reactions of mobile species with defects in silica are significantly conditioned by the characteristic structural disorder of the solid.<sup>3,15,16,31</sup> Hence, the study of these processes is interesting also from a fundamental point of view as a probe of the effects of disorder in amorphous solids.

To contribute to the clarification of these issues, we report here experiments aimed at studying the postirradiation stability of the defects induced in silica by  $\gamma$  irradiation as a function of the dose administered to the material.

**Materials and Methods**

The experiments were performed on  $2 \times 2 \times 5$  mm Infrasil 1301 (I301) fused silica samples supplied by Heraeus Quarzglas GmbH. This material is a type I  $\text{SiO}_2$  manufactured by fusion and quenching of natural quartz powder, with a typical

\* Corresponding author.

<sup>†</sup> Dipartimento di Scienze Fisiche ed Astronomiche.

<sup>‡</sup> Dipartimento di Ingegneria Nucleare.

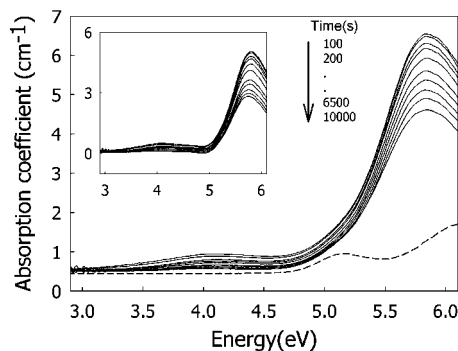


**Figure 1.** Absorption spectra measured in I301 fused silica at different delays after the end of  $\gamma$  irradiation (solid lines). Inset: difference spectra at the same times calculated by subtracting the absorption spectrum of the as-grown sample (dashed line in the main panel).

concentration of impurities of  $\sim 20$  ppm by weight and low [OH] content ( $\sim 8$  ppm).<sup>32</sup> Moreover, samples feature a concentration of Si–H groups exceeding  $10^{18}$   $\text{cm}^{-3}$  as estimated via Raman spectroscopy by the manufacturer.<sup>33</sup> The  $E'_\gamma$  centers were absent in the as-grown samples, as checked by electron spin resonance (ESR) measurements. The main signal in the vis–UV absorption spectrum of the as-grown sample is the  $B_{2\beta}$  absorption band at 5.1 eV due to 2-fold coordinated Ge impurities, present in  $\sim 10^{16}$   $\text{cm}^{-3}$  concentration in this material.<sup>1,34,35</sup> Preliminary measurements in the vacuum UV spectral range reveal the presence of the 7.6 eV absorption band related to oxygen vacancies ( $\equiv\text{Si}-\text{Si}\equiv$ ).<sup>34</sup> From the amplitude of the band and the known absorption cross section,<sup>34</sup> we estimate in the as-grown Infrasil 1301 samples a concentration of  $[\equiv\text{Si}-\text{Si}\equiv] = (3 \pm 1) \times 10^{17}$   $\text{cm}^{-3}$  (taking into account sample-to-sample fluctuations).

$\gamma$  irradiations were performed at 300 K by a  $^{60}\text{Co}$  source featuring a  $\sim 1$  kGy/h dose rate. Laser irradiations, also at 300 K, were performed by using the fourth harmonic at 4.7 eV of a Q-switched Nd:YAG laser (pulse duration 5 ns, repetition frequency 1 Hz, 40 mJ/cm<sup>2</sup> energy density per pulse). We measured the OA spectra of the samples before any treatment and at different delays after the end of  $\gamma$  or laser irradiation by a single-beam Avantes optical fiber spectrophotometer, equipped by a D<sub>2</sub> lamp source and a charge-coupled device (CCD) detector sensitive in the 200–400 nm range and allowing a time resolution of the spectra of 1 s. ESR spectra were measured with a Bruker EMX spectrometer working at 9.8 GHz (X-band). The microwave power was set to  $P = 8 \times 10^{-4}$  mW and the modulation amplitude to 0.01 mT to avoid saturation and distortion effects in revealing the induced  $E'_\gamma$  centers. Absolute defect concentrations were obtained from comparison of the signal with a reference silica sample whose defect concentration was measured by the spin–echo decay method.<sup>36</sup> The absolute accuracy of the so-obtained concentration estimates is 20%, while the relative precision is 10%. Infrared absorption measurements were performed by a Bruker Vertex 70 Fourier transform single-beam absorption spectrometer, equipped by a medium-IR light global source.

## Results and Discussion

An as-grown I301 sample was irradiated with a 4.9 kGy dose of  $\gamma$  radiation by exposing it to the  $^{60}\text{Co}$  source for  $\Delta t = 1.7 \times 10^4$  s. After 100 s from the end of irradiation, we started monitoring the OA spectrum of the sample for a few hours (Figure 1). The difference spectra (inset of Figure 1) with respect to the as-grown absorption profile evidence the absorption band peaked at 5.8 eV associated with the  $E'_\gamma$  centers,<sup>1,2,34</sup> induced

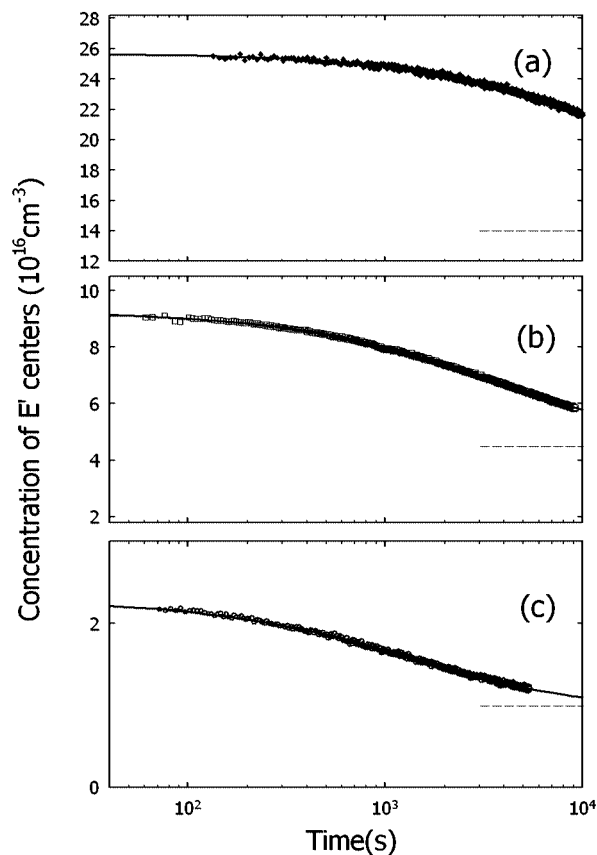


**Figure 2.** Postirradiation kinetics of the concentration of  $E'_\gamma$  centers after irradiation of I301 silica with a 79 kGy (a), 4.9 kGy (b), and 0.6 kGy (c) dose of  $\gamma$  radiation. Dotted lines represent the asymptotic concentrations of defects as estimated by ESR measurements one month after irradiation. The solid lines are best fit curves obtained with the procedure described in the text. The dotted red line in panel b is a fitting curve obtained by considering the combined effect of reactions 1 and 6.

by  $\gamma$  irradiation. We observe that the amplitude of the induced 5.8 eV band progressively decays after the end of exposure, from the initial value of 5  $\text{cm}^{-1}$  measured 10<sup>2</sup> s after irradiation, to 3  $\text{cm}^{-1}$  measured after 10<sup>4</sup> s. Aside from the 5.8 eV signal,  $\gamma$  irradiation induces a wide absorption band peaked around 4 eV which decays in the postirradiation stage as well. This is a minor signal which has been ascribed to Ge or Al impurities present in fused silica<sup>37</sup> and will not be considered in the following.

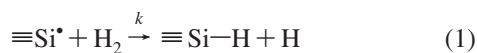
From the area of the 5.8 eV band and the oscillator strength associated with the  $E'_\gamma$  centers,<sup>38</sup> we estimate the concentration  $[E']$  of the defects, which is plotted in Figure 2b as a function of time. The origin of the time scale corresponds to the end of irradiation. We see that  $[E']$  decreases from  $9.0 \times 10^{16}$   $\text{cm}^{-3}$  at  $t = 10^2$  s to  $5.8 \times 10^{16}$   $\text{cm}^{-3}$  at  $t = 10^4$  s. Since the decay is still in progress after 10<sup>4</sup> s from the end of irradiation, the most convenient way to accurately estimate the asymptotic concentration of  $E'_\gamma$  is by ex situ OA or ESR measurements performed about one month after the experiment. Asymptotic concentrations reported in the present paper were obtained by ESR, since the latter allows for a higher accuracy at low ( $\sim 10^{16}$   $\text{cm}^{-3}$ ) defect concentrations. In this way we obtained  $[E']_\infty = 4.5 \times 10^{16}$   $\text{cm}^{-3}$ . This measurement was repeated one year and two years after irradiation, yielding the same value within experimental uncertainty. Hence, roughly 50% of the  $E'_\gamma$  centers initially induced by  $\gamma$  radiation disappear in the postirradiation stage.

We repeated the same experiment at two different irradiation doses, 79 kGy ( $\Delta t = 2.8 \times 10^5$  s) and 0.6 kGy ( $\Delta t = 2.2 \times$

$10^3$  s), so obtaining the kinetics reported in parts a and c, respectively, of Figure 2. In these experiments we measured  $[E']_{\infty} = 1.4 \times 10^{17} \text{ cm}^{-3}$  and  $[E']_{\infty} = 1.0 \times 10^{16} \text{ cm}^{-3}$ . By comparing the concentration of  $E'_{\gamma}$  immediately after the end of irradiation with the asymptotic concentration  $[E']_{\infty}$ , we see that the postirradiation decay involves roughly half of the initially induced defects at every investigated dose.

Data in Figures 1 and 2 show that the  $E'_{\gamma}$  centers induced by  $\gamma$  radiation spontaneously undergo partial annealing at room temperature in a time scale of hours starting from the end of irradiation. This result contrasts with the generally agreed stability of  $E'_{\gamma}$  centers at room temperature and demonstrates that postirradiation decay effects can strongly influence radiation-induced damage. Only a few papers have previously reported similar results.<sup>21</sup>

In the literature, the annealing of radiation-induced defects is usually explained as a consequence of their reactions with diffusing mobile species, either made available by irradiation or already present in the as-grown material. At room temperature,  $\text{H}_2$  is usually considered as the only chemical species that appreciably diffuses in silica<sup>3,6,8,9,14,15,24</sup> and is able to passivate the  $E'_{\gamma}$  center by the reaction<sup>4-10,14,16,24</sup>



where the hydrogen atom at the right side is supposed to migrate and passivate another  $E'_{\gamma}$  center. To put forward a quantitative analysis of the experimental decay kinetics, we begin by briefly reviewing the standard mathematical treatment of the kinetics of a bimolecular reaction. Reaction 1, in the stationary-state approximation for atomic hydrogen,<sup>3,16,39</sup> is described by the following rate equation:

$$\frac{d[E']}{dt} = 2 \frac{d[\text{H}_2]}{dt} = -2k[E'][\text{H}_2] \quad (2)$$

where the reaction constant  $k$  depends on the temperature by an Arrhenius equation<sup>16</sup>

$$k = k_0 \exp(-E_a/k_B T) \quad (3)$$

$k_0$  and  $E_a$  being the pre-exponential factor and the activation energy of the reaction, respectively. A recent experiment clarified the reaction properties of  $E'_{\gamma}$  centers induced by UV laser irradiation with diffusing  $\text{H}_2$ .<sup>16</sup> It was found that the kinetics of reaction 1 is reaction-limited rather than diffusion-limited and is well described by eq 2 only if one introduces a statistical distribution of  $E_a$ , Gaussian-shaped with a center in  $E_{a,0} = 0.38 \pm 0.01$  eV and width  $\sigma_0 = 0.05 \pm 0.01$  eV, the pre-exponential factor being  $k_0 \approx 3 \times 10^{-14} \text{ cm}^3 \text{ s}^{-1}$ .<sup>16,31</sup> Such a statistical distribution (which implies  $k$  to be distributed as well) accounts for the typical disorder of the amorphous matrix in which the diffusion-reaction process takes place.

Neglecting for the moment the statistical distribution of  $k$ , we can conveniently analyze the kinetics of Figure 2 by considering the solution of eq 2:<sup>40</sup>

$$[E']_t = \frac{[E']_{\infty}}{1 - \frac{[E']_{t_0} - [E']_{\infty}}{[E']_{t_0}} \exp(-k[E']_{\infty}(t - t_0))} \quad (4)$$

where  $t_0$  is the time at which the first measurement was performed and the total variation of  $[E']$ ,  $\Delta[E'] = [E']_{t_0} - [E']_{\infty}$ , equals 2 times the initial hydrogen concentration:  $\Delta[E'] = 2[\text{H}_2]_{t_0}$ . Now we write eq 4 as

$$z = \frac{[E']_{t_0}}{[E']_{t_0} - [E']_{\infty}} \left(1 - \frac{[E']_{\infty}}{[E']_t}\right) = \exp(-k\tau) \quad (5)$$

where we have defined  $\tau = [E']_{\infty}(t - t_0)$ . Since  $[E']_{\infty}$  is known from ESR measurements, the quantity  $z(\tau)$  defined by eq 5 can be calculated from experimental data.  $z(\tau)$  is an adimensional quantity between 0 and 1 that accounts for the degree of completion of the kinetics. The advantage of representing experimental data in this way is that every kinetic characterized by a given reaction constant  $k$  should be simply represented by a given exponential, independent of the initial conditions.

$z(\tau)$  is plotted in Figure 3 for each of the kinetics in Figure 2. Data in Figure 3 clearly show that the decay kinetics become progressively slower with increasing dose, meaning that the three kinetics cannot be accounted for by a single value of the (mean) reaction constant  $k$ . In contrast, the observed  $k$  decreases with growing irradiation dose. The slight disagreement between the shape of experimental curves and the theoretical ones is due to the fact that eq 5 neglects the statistical distribution of  $k$ . For comparison, we measured the postirradiation kinetics of  $E'_{\gamma}$  centers induced by irradiation of an as-grown I301 sample with 2000 UV laser pulses. The corresponding  $z(\tau)$  is reported in Figure 3 as well. Previous experiments demonstrated that Nd:YAG laser irradiation of fused silica at room temperature induces the rupture of pre-existing hydride (Si-H) precursors, thus generating  $E'_{\gamma}$  centers together with hydrogen atoms. The latter dimerize in  $\text{H}_2$  that diffuses and passivates the generated  $E'_{\gamma}$  centers in the postirradiation stage by reaction 1.<sup>14,16,31</sup> From Figure 3 it is apparent that the postirradiation kinetics observed after 0.6 kGy  $\gamma$  irradiation closely resembles that observed upon laser exposure. On the basis of this analogy, we guess that the decay of  $E'_{\gamma}$  induced by 0.6 kGy  $\gamma$  radiation is due to reaction with  $\text{H}_2$ . Also, this leads to the hypothesis that both the generation of  $E'_{\gamma}$  and the production of radiolytic hydrogen available for reaction 1, occur under a low dose of  $\gamma$  irradiation by the same mechanism that is triggered by UV photons, i.e., the rupture of Si-H precursors.

Since the activation energy for reaction 1 is distributed around  $E_{a,0}$  with  $\sigma_0$  width, while its characteristic pre-exponential factor is  $k_{0,0}$ ,<sup>16</sup> one can define a typical range of  $k$  values for the process, limited by  $k_{0,0} \exp[-(E_{a,0} \pm \sigma_0)/k_B T]$ . This allows a region in Figure 3 to be individuated, consistent with the passivation of  $E'_{\gamma}$  by diffusing  $\text{H}_2$ . As expected, we see that

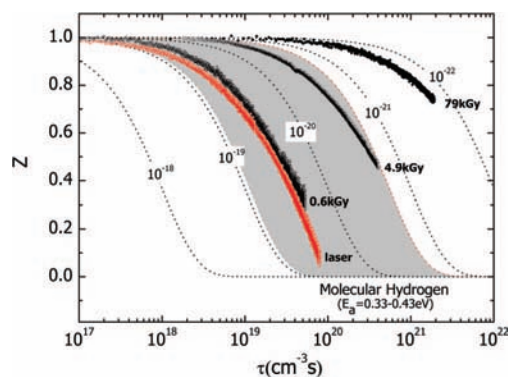


**Figure 3.** Quantity  $z$  defined by eq 5 as a function of  $\tau = [E']_{\infty}(t - t_0)$ , calculated for the decay kinetics observed after 0.6, 4.9, and 79 kGy doses of  $\gamma$  irradiation and after laser irradiation with 2000 Nd:YAG laser pulses. Dashed lines are theoretical exponential curves, as predicted by eq 5, calculated for several values of  $k$  (reported in units of  $\text{cm}^3 \text{ s}^{-1}$  along the curves). The gray region represents the interval of theoretical curves, delimited by the  $k$  values calculated by using eq 3 with  $k_0 = k_{0,0}$  and  $E_a = E_{a,0} - \sigma_0$  and  $E_{a,0} + \sigma_0$ , characteristic of reaction 1.<sup>16,31</sup>

**TABLE 1: Irradiation Dose, Concentration of  $E'_\gamma$  Centers at the End of  $\gamma$  Irradiation, and Mean Value and Width of the Distribution of Activation Energies Obtained by Fitting the Kinetics in Figure 2 by a Linear Combination of Solutions of Eq 2 Weighted by a Gaussian Distribution of  $E_a$**

dose (kGy)	$[E'] (t=0)$ ( $\text{cm}^{-3}$ )	$\langle E_a \rangle$ ( $\text{H}_2$ ) (eV)	$\sigma$ (eV)
0.6	$2.3 \times 10^{16}$	$0.36 \pm 0.02$	$0.03 \pm 0.01$
4.9	$9.2 \times 10^{16}$	$0.42 \pm 0.02$	$0.03 \pm 0.01$
79.0	$2.6 \times 10^{17}$	$0.50 \pm 0.02$	$0.04 \pm 0.01$

both the decay kinetics after 0.6 kGy and that observed after laser irradiation fall within this region. The kinetics measured after 4.9 kGy irradiation, though being slower, is still within the boundaries of the  $\text{H}_2$  region. Finally, the kinetics measured after 79 kGy irradiation is well outside the typical  $k$  interval of reaction 1.

Similar conclusions can be drawn by a more quantitative analysis that includes the effects of the statistical distribution: to this aim, we least-squares fitted the three kinetics in Figure 2 with a linear combination of expressions like eq 4, with  $t_0 = 0$ , weighted by a Gaussian distribution of  $E_a$ , with center  $\langle E_a \rangle$  and width  $\sigma$ . In each fit, the asymptotic concentration of  $E'$  was fixed (within a 10% uncertainty) to the value obtained from ESR measurements. Furthermore, since the rate equation depends only on  $k$ , measurements at a single temperature are unable to distinguish the contributions of  $E_a$  and  $k_0$  to  $k$ . Hence, to estimate  $E_a$ , in the fitting procedure we fixed the pre-exponential factor  $k_0$  in eq 3 to  $k_{0,0} = 3 \times 10^{-14} \text{ cm}^3 \text{ s}^{-1}$ , i.e., the characteristic value of reaction 1.<sup>16</sup> With this procedure, we obtained estimates of three parameters,  $[E'] (t=0)$ ,  $\langle E_a \rangle$ , and  $\sigma$ , which are reported in Table 1.

We see that the measured mean activation energy at the lowest dose is consistent with the previously known value for reaction 1:  $E_{a,0} = 0.38 \pm 0.01 \text{ eV}$ .<sup>16</sup> Then  $\langle E_a \rangle$  as obtained by the fits grows with dose up to 0.50 eV, this being consistent with the observed decrease of the reaction constant  $k$ . In what concerns the width of the distribution, it appears to grow as well, even if it remains consistent with  $\sigma_0$  within our experimental error.

A possible interpretation of these findings is that the growth with dose of the measured  $E_a$  is due to the selection during irradiation of  $E'_\gamma$  centers featuring progressively higher activation energies for reaction 1. Specifically, let us suppose that the  $E'_\gamma$  centers generated by  $\gamma$  photons feature the Gaussian distribution of  $E_a$  already known from previous works,<sup>16,31</sup> peaked at  $E_{a,0}$  and with  $\sigma_0$  width. Then, as the irradiation dose grows, the irradiation time becomes comparable with the typical time scale of the decay. Since reaction 1 is expected to take place also during  $\gamma$  irradiation, one can argue that the most reactive subset of the total population of  $E'_\gamma$  centers has already reacted with  $\text{H}_2$  at the end of exposure, so that we are left with a subset of the Gaussian distribution including only the least reactive defects. In this sense, the values in Table 1 should be interpreted as *effective* values characteristic of the portion of defects remaining at the end of irradiation. Also, this selective effect is further enhanced by the fact that experimental observations begin about  $10^2 \text{ s}$  after the end of exposure, thus being unable to evidence the fastest portion of the decay kinetics and thus increasing the effective  $E_a$ . This interpretation allows understanding of the behavior of the two kinetics after 0.6 and 4.9 kGy irradiation: their  $E_a$  values in Table 1 both fall within one  $\sigma_0$  (0.05 eV) from the expected value  $E_{a,0}$  (0.38 eV) for reaction with  $\text{H}_2$ , but the kinetics after 0.6 kGy is significantly faster ( $\langle E_a \rangle = 0.36 \text{ eV}$ ) than that after 4.9 kGy ( $\langle E_a \rangle = 0.42 \text{ eV}$ ).

In what concerns the kinetics after the 79 kGy dose, however, this scheme appears quite unlikely. In fact, a concentration of annealed defects of  $\Delta[E'] = 1.2 \times 10^{17} \text{ cm}^{-3}$ , featuring a mean activation energy of 0.50 eV (see Table 1), would be supposedly selected (by the annealing taking place during irradiation) from the whole population of defects, featuring a mean activation energy of  $E_{a,0} = 0.38 \text{ eV}$ . Since  $0.50 \text{ eV} - E_{a,0} > 2\sigma_0$ , this could be possible only if the total concentration of induced defects were at least  $100\Delta[E']$ , too high to be compatible with any experimental evidence on the generation of  $E'_\gamma$ .

Therefore, another model is needed to explain the kinetics after 79 kGy. A simple possible hypothesis is that  $E'_\gamma$  centers formed from different precursors feature different reaction properties with  $\text{H}_2$ . In particular, let us suppose that Si-H is the prevalent precursor for  $E'_\gamma$  centers at low  $\gamma$  doses and that this process rapidly saturates with dose, while most of the defects generated by 79 kGy  $\gamma$  radiation arise from transformation of a second precursor, such as the oxygen vacancy.<sup>1,41</sup> It is conceivable that  $E'_\gamma$  generated from different precursors may feature different activation energies for reaction 1, 0.38 and 0.50 eV (assuming the same pre-exponential factor), due to different environments of the defect.

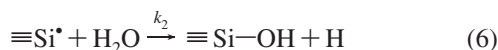
While the present data do not allow this scheme to be conclusively ruled out, an alternative explanation exists, possibly simpler, which should be taken into consideration to explain the data for the 79 kGy irradiation. To illustrate it, we first observe that the mean activation energies reported in Table 1 were estimated by supposing  $k_{0,0}$  as the pre-exponential factor for the reaction constant. If we rule out the hypothesis that the passivation of  $E'_\gamma$  is due to  $\text{H}_2$ , we can tentatively propose another mobile species X as the annealing agent. If X reacted with  $E'_\gamma$  by a diffusion-limited reaction, as described by Waite's theory,<sup>42</sup> the activation energy for the reaction should equal that for diffusion of X in silica, while the pre-exponential factor of  $k$  would be  $k_{0,w} = 4\pi r_0 D_0$ , where  $r_0$  is the capture radius, expected to be on the order of a few  $10^{-8} \text{ cm}$ , and  $D_0$  is the pre-exponential factor for diffusion of the mobile species. Now, assuming typical values for silica,  $r_0 = 5 \times 10^{-8} \text{ cm}$  and  $D_0 = 10^{-4} \text{ cm}^2 \text{ s}^{-1}$ ,<sup>43</sup> we obtain  $k_{0,w} = 6.3 \times 10^{-11} \text{ cm}^3 \text{ s}^{-1}$ .<sup>44</sup>

We repeated the fit of the kinetics observed after the 79 kGy irradiation by now fixing the pre-exponential factor to  $k_{0,w}$  instead of  $k_{0,0}$ . In this way we obtained a new estimate,  $\langle E_a \rangle (\text{X}) = 0.70 \text{ eV}$ . This value is very close to that reported in the literature for diffusion of  $\text{H}_2\text{O}$  in silica (0.72 eV).<sup>43</sup> Hence, it appears that the postirradiation decay observed after 79 kGy irradiation is consistent with the  $E'_\gamma$  centers being passivated by a diffusion-limited reaction with  $\text{H}_2\text{O}$ .

It is worth stressing that in our reasoning we are making two assumptions: (a) the Arrhenius expression of the water diffusion constant in silica,  $D_{\text{H}_2\text{O}} (\text{cm}^2 \text{ s}^{-1}) = 1.3 \times 10^{-4} \exp(-0.72 \text{ eV} / k_B T)$ , obtained from measurements in the 200–1200 °C range,<sup>43</sup> can be extrapolated down to room temperature; (b) at room temperature  $\text{H}_2\text{O}$  diffuses in silica “freely”; i.e.,  $\text{H}_2\text{O}$  reacts only with  $E'_\gamma$  centers but not with ordinary Si-O-Si bonds. In this respect, it is known that water diffusion in  $\text{SiO}_2$  at higher temperatures is strongly conditioned by reactions with the unperturbed silicon-oxygen network,<sup>43,45</sup> so that one observes an *effective* diffusion coefficient  $D_{\text{eff}}$ , different from  $D_{\text{H}_2\text{O}}$  and generally time-dependent. Even when a local equilibrium with the  $\text{SiO}_2$  matrix is established,  $D_{\text{eff}}$  is a function of the Si-OH concentration in the matrix.<sup>43,45</sup> However, since reactions of  $\text{H}_2\text{O}$  with  $\text{SiO}_2$  have been actually demonstrated only at temperatures higher than  $\sim 200 \text{ °C}$ ,<sup>43,46</sup> we are assuming these effects to be negligible at room temperature. Under this hypothesis, the

parameter controlling the reaction kinetics of H<sub>2</sub>O with E'<sub>γ</sub> is expected to be the ordinary diffusion coefficient D<sub>H<sub>2</sub>O</sub>, as opposed to D<sub>eff</sub>, which takes into account the reaction with SiO<sub>2</sub>, whose effects are supposedly negligible, at least within the experimental time scale.<sup>47</sup>

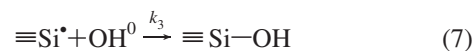
We are finally led to another interpretation scheme. γ-ray irradiation of 79 kGy, differently from laser exposure, makes available water aside from hydrogen. The irradiation being sufficiently long, passivation of E'<sub>γ</sub> centers due to reaction with H<sub>2</sub> takes place almost completely during irradiation, while the slow annealing observed in the postirradiation stage can be ascribed to reaction with H<sub>2</sub>O of the E'<sub>γ</sub> centers which have survived recombination with hydrogen:



where, like in reaction 1, the hydrogen atom at the right side is supposed to passivate another E' center.

Provided that the annealing of E'<sub>γ</sub> centers induced by a low dose (0.6 kGy) of irradiation can be completely ascribed to H<sub>2</sub> diffusion (featuring  $\langle E \rangle = 0.38$  eV and  $k_0 = 3 \times 10^{-14}$  cm<sup>3</sup> s<sup>-1</sup>) and that of defects induced by a high dose (79 kGy) of irradiation can be explained by reaction 6 (featuring  $\langle E \rangle = 0.70$  eV and  $k_0 = 6.3 \times 10^{-11}$  cm<sup>3</sup> s<sup>-1</sup>), one should check whether the intermediate case, namely, the kinetics observed after 4.9 kGy irradiation, can be described as a combination of the two processes. To this purpose, we verified that data in Figure 2b can be satisfactorily reproduced by a numerically calculated solution (dashed curve) of the system of the two chemical rate equations associated with reactions 1 and 6. In detail, a good fitting curve was obtained with the following initial concentrations of reactants, [H<sub>2</sub>]<sub>0</sub> = 1.0 × 10<sup>16</sup> cm<sup>-3</sup>, [H<sub>2</sub>O]<sub>0</sub> = 1.6 × 10<sup>16</sup> cm<sup>-3</sup>, and with the following two distributions of activation energies,  $\langle E \rangle_1 = 0.39$  eV and  $\sigma_1 = 0.03$  eV (associated with H<sub>2</sub>) and  $\langle E \rangle_2 = 0.65$  eV and  $\sigma_2 = 0.03$  eV (associated with H<sub>2</sub>O). We see that  $\langle E \rangle_1$  is reasonably close to the activation energy of 0.38 eV associated with process 1,<sup>16</sup> as well as to the activation energy found from the annealing kinetics after 0.6 kGy irradiation. Similarly,  $\langle E \rangle_2$  is close to the value of 0.70 eV found above from the annealing kinetics observed after 79 kGy, supposedly due to diffusion and reaction of H<sub>2</sub>O. Hence, this result self-consistently completes the scheme depicted so far by demonstrating that the postirradiation kinetics measured after the intermediate dose is due to the combined effect of hydrogen- and water-controlled reactions.

In the literature, a significant reduction of the concentration of E'<sub>γ</sub> centers associated with water diffusion has been observed only at temperatures higher than ~250 °C, so that water has been considered to be basically immobile at room temperature.<sup>21</sup> However, the present results apparently contrast with these findings, suggesting that even at room temperature the reaction between E'<sub>γ</sub> and H<sub>2</sub>O could be relevant to understand the long-term decay of the induced defects. On the other side, isolated OH<sup>0</sup> groups have been proposed to exist in silica as a relatively fast diffusing species.<sup>21,48</sup> In fact, the ESR signal of the paramagnetic OH<sup>0</sup> radical, consisting in a doublet with 4.3 mT splitting,<sup>48</sup> was observed upon X-ray irradiation at 77 K. Then, it started to decay by heating above  $T > 200$  K, presumably due to diffusion and recombination with other species. The present results do not allow the conclusive discrimination of the effect of water diffusion from that of OH<sup>0</sup> diffusion; namely, the long-term decay of E'<sub>γ</sub> centers after 79 kGy irradiation may be due to a modified version of reaction 6 containing OH<sup>0</sup> instead of H<sub>2</sub>O:



Further experiments are needed to distinguish reaction 6 from reaction 7. The observation of a transient ESR signal with the reported spectral features, decaying during the postirradiation stage after 79 kGy irradiation, may yield conclusive proof of the involvement of OH<sup>0</sup> diffusion. Finally, it is worth noting that, in principle, an advantage of reaction 7 over process 6 is that OH<sup>0</sup> groups are expected to be much more reactive than H<sub>2</sub>O due to their paramagnetic nature: if reaction 7 applies, then the value of  $\langle E_a \rangle(X) = 0.70$  eV found by our fitting procedure should be interpreted as the activation energy for the diffusion of OH<sup>0</sup> groups in SiO<sub>2</sub>.

Water may be formed by reaction of radiolytic hydrogen with oxygen atoms (O<sup>0</sup>) made available by knock-on events on the unperturbed matrix, or alternatively it may be already dissolved in the as-grown material. It is worth noting that the direct recombination of E'<sub>γ</sub> with diffusing O<sup>0</sup> can be ruled out. Indeed, such a process should form the nonbridging oxygen hole centers ( $\equiv\text{Si}-\text{O}\cdot$ ):<sup>20</sup> we verified that these defects are absent within a 10<sup>15</sup> cm<sup>-3</sup> concentration in irradiated specimens as inferred by the lack of their 1.9 eV emission band under laser excitation at 4.8 eV.<sup>1,49</sup> On the other side, OH<sup>0</sup> groups needed for reaction 7 may be formed by radiolysis of water molecules or of Si-OH groups or by reaction of H with O<sup>0</sup> atoms generated by knock-on processes.

In Figure 4 we compare the present results to those reported in a seminal paper by Griscom where a similar experiment was performed on high-OH (1200 ppm) synthetic silica specimens irradiated with different doses of γ radiation.<sup>21</sup> ESR measurements of the concentration of E'<sub>γ</sub> centers at different delays (>10<sup>3</sup> s) from the end of irradiation at room temperature showed a postirradiation decay of the defects occurring on a time scale ranging from 10<sup>3</sup> to 10<sup>8</sup> s. The portion of defects annealed by the postirradiation decay turned out to strongly depend on the dose. Indeed, as apparent from Figure 4, the defects induced by 27 kGy irradiation were almost completely annealed after ~10<sup>8</sup> s, while only ~30% of those induced by 260 kGy irradiation decayed in the postirradiation stage, and the defects induced by 4400 kGy irradiation were basically stable in the postirradiation stage. Despite the difference in irradiation doses and dose rates (1.2 Gy/s in ref 21 and 0.28 Gy/s in the present experiment), the comparison seems to suggest that postirradiation decay processes are a very general issue strongly affecting the stability of E'<sub>γ</sub> centers at room temperature. On the other side, the kinetics reported in ref 21 are qualitatively similar to ours only in the short time range ( $t < 10^4$  s), while being in strong contrast as concerns the asymptotic behavior. In fact, in

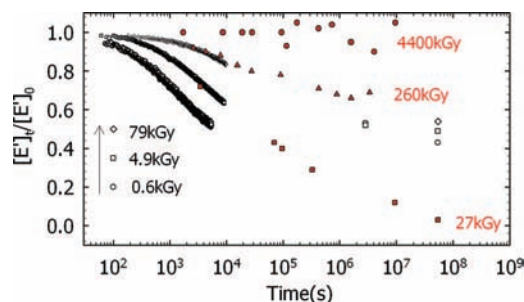


**Figure 4.** Open symbols: fractional concentration of E'<sub>γ</sub> centers, [E']<sub>t</sub>/[E']<sub>0</sub>, as calculated from data in Figure 2. Full red points: decay kinetics of E'<sub>γ</sub> centers after γ irradiation at three different doses, taken from ref 21.

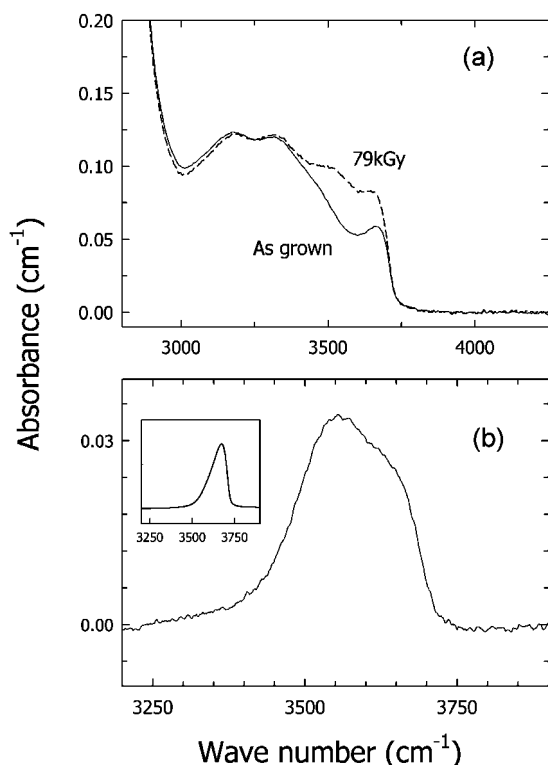


**Figure 5.** (a) Infrared absorption spectrum of an as-grown fused silica sample (continuous line) and of the sample irradiated by 79 kGy  $\gamma$  irradiation (dashed line). (b) Difference spectrum between the two signals in panel a. Inset of panel b: characteristic signal due to the Si–OH stretching vibrational mode, as measured in a wet Suprasil silica sample,<sup>32</sup> with a high concentration of Si–OH groups.

the present experiment performed on low-OH silica the portion of decaying defects is about 50% for all three investigated doses (see Figure 2). Further experiments are needed to clarify the reason behind this difference, which may be due, for instance, to different long-term decay pathways for the  $E'_\gamma$  centers active in the two materials, related to different initial concentrations of slowly diffusing species ( $H_2O$  or  $OH^0$ ).

Both reactions 6 and 7 are expected to cause an increase of the concentration of Si–OH groups. This prediction was experimentally tested by performing IR measurements on as-grown and irradiated silica samples (Figure 5) one month after the end of irradiation. The IR absorption profile of the as-grown sample features a weak peak at  $3670\text{ cm}^{-1}$  due to the stretching vibrational mode of Si–OH groups.<sup>50–52</sup> Furthermore, the broad signal observed in the region between  $3000$  and  $3600\text{ cm}^{-1}$  (with main peaks at  $3180$  and  $3320\text{ cm}^{-1}$  and a shoulder near  $3425\text{ cm}^{-1}$ ) can be decomposed into three Gaussian contributions at  $3200$ ,  $3342$ , and  $3450\text{ cm}^{-1}$  by a deconvolution procedure. According to the literature data,<sup>52</sup> the two signals at  $3200$  and  $3425$ – $3450\text{ cm}^{-1}$  have to be attributed to  $H_2O$  molecules. Hence, on the basis of the known molar extinction coefficient of the  $3425$ – $3450\text{ cm}^{-1}$  band,  $81\text{ (L cm}^{-1}\text{)/mol(H}_2\text{O)}$ ,<sup>53</sup> we estimate a concentration of  $[H_2O] = (2.1 \pm 0.5) \times 10^{17}\text{ cm}^{-3}$  dissolved in the as-grown material. This value is sufficiently high to suggest that water required for reaction 6 is already present in the as-grown material.

As apparent from Figure 5, 79 kGy  $\gamma$  irradiation induces measurable alterations in this region of the infrared absorption spectrum. In contrast, we observed no significant variations of the absorption spectrum upon 0.6 kGy or 4.9 kGy  $\gamma$  irradiation. The difference spectrum shows the growth of a signal with a main peak at  $3550\text{ cm}^{-1}$  and a shoulder near  $3650\text{ cm}^{-1}$ . Its

overall shape is composite and broader than the ordinary  $3670\text{ cm}^{-1}$  peak of Si–OH groups usually observed in as-grown silica with high Si–OH content (inset). In the literature, a signal at  $3510\text{ cm}^{-1}$ , near the main peak of our difference spectrum, has been attributed to the stretching of Si–OH pairs linked by a hydrogen bond.<sup>52</sup> Data in Figure 5 suggest that  $\gamma$  irradiation induces the growth of several OH-related species. Even if the present measurements are insufficient to clarify the mechanisms by which different varieties of Si–OH groups may be formed, the observed increase of the absorption in this region points to either eq 6 or eq 7 as the most probable mechanism causing the decay of  $E'_\gamma$  centers after a high dose of  $\gamma$  irradiation. Also, the absence of evident negative contributions at  $3200$  and  $3425$ – $3450\text{ cm}^{-1}$  in the difference spectrum, which should be expected if  $H_2O$  were involved in reaction 6, suggests now that reaction 7 is more likely than reaction 6 to be the active annealing mechanism of the  $E'_\gamma$  center. However, a more complete study of the dose dependence of the irradiation-induced alterations of the IR absorption spectrum is mandatory to provide conclusive evidence.

Finally, while it is difficult to extract from the difference spectrum the absolute concentration of induced Si–OH groups, its order of magnitude can be assessed by considering that an absorption coefficient of  $0.035\text{ cm}^{-1}$  corresponds to a concentration  $\Delta[\text{Si–OH}] \approx 1 \times 10^{17}\text{ cm}^{-3}$  by using the peak molar extinction coefficient of  $77.5\text{ L mol}^{-1}\text{ cm}^{-1}$  associated with the ordinary Si–OH signal.<sup>51</sup> Such an order of magnitude is qualitatively consistent with the decay  $\Delta[E'_\gamma] = 1.2 \times 10^{17}\text{ cm}^{-3}$  measured after irradiation with 79 kGy.

## Conclusions

We studied the postirradiation room temperature annealing of  $E'_\gamma$  centers induced in amorphous  $\text{SiO}_2$  by  $\gamma$  irradiation. We observe that a significant portion of the defects decay after the end of exposure. The rate of the decay progressively slows with increasing exposure time and accumulated dose. The  $E'_\gamma$  centers induced by irradiation with 0.6 kGy  $\gamma$  irradiation are most likely annealed by reaction with mobile  $H_2$  of radiolytic origin, as previously observed for  $E'_\gamma$  induced by UV laser irradiation. In contrast, the decay kinetics of  $E'_\gamma$  induced by 79 kGy irradiation can be interpreted as due to reaction of the defect with another chemical species featuring a much slower diffusion constant. From the quantitative analysis of the kinetics, we propose water-related species ( $H_2O$  or  $OH^0$ ) to be responsible for the slow annealing observed in this regime. This conclusion is supported by the observation by IR measurements of the growth of Si–OH groups upon irradiation. Finally, the decay kinetics of  $E'_\gamma$  centers induced by an intermediate 4.9 kGy dose is consistent as well with our interpretation model: indeed, it can be explained as being due to a combination of passivation by  $H_2$  and by the water-related species.

**Acknowledgment.** We acknowledge partial financial support received from the project P.O.R. Regione Sicilia–Misura 3.15–Sottoazione C. We thank the members of the LAMP group (<http://www.fisica.unipa.it/amorphous>) for support and stimulating discussions.

## References and Notes

- (1) Pacchioni, G.; Skuja, L.; Griscom, D. L., Eds. *Defects in  $\text{SiO}_2$  and Related Dielectrics: Science and Technology*; Kluwer Academic Publishers: Hingham, MA, 2000.
- (2) Nalwa, H. S., Ed. *Silicon-Based Materials and Devices*; Academic Press: New York, 2001.
- (3) Griscom, D. L. *J. Non-Cryst. Solids* **1984**, *68*, 301.

- (4) Li, Z.; Fonash, S. J.; Poindexter, E. H.; Harmatz, M.; Rong, F.; Buchwald, W. R. *J. Non-Cryst. Solids* **1990**, *126*, 173.
- (5) Bobyshev, A. A.; Radtsig, V. A. *Kinet. Katal.* **1990**, *31*, 931.
- (6) Imai, H.; Arai, K.; Hosono, H.; Abe, Y.; Arai, T.; Imagawa, H. *Phys. Rev. B* **1991**, *44*, 4812.
- (7) Kuzuu, N.; Komatzu, Y.; Murahara, M. *Phys. Rev. B* **1991**, *44*, 9265.
- (8) Edwards, A. H.; Pickard, J. A.; Stahlbush, R. E. *J. Non-Cryst. Solids* **1994**, *179*, 148.
- (9) Vitiello, M.; Lopez, N.; Illas, F.; Pacchioni, G. *J. Phys. Chem. A* **2000**, *104*, 4674.
- (10) Afanas'ev, V. V.; Stesmans, A. *J. Phys.: Condens. Matter* **2000**, *12*, 2285.
- (11) Lou, V.; Sato, R.; Tomozawa, M. *J. Non-Cryst. Solids* **2003**, *315*, 13.
- (12) Sato, R.; Tomozawa, M. *J. Non-Cryst. Solids* **2004**, *343*, 26.
- (13) Saito, K.; Ito, M.; Ikushima, A.; Funahashi, S.; Imamura, K. *J. Non-Cryst. Solids* **2004**, *347*, 289.
- (14) Messina, F.; Cannas, M. *J. Phys.: Condens. Matter* **2005**, *17*, 3837.
- (15) Kajihara, K.; Skuja, L.; Hirano, M.; Hosono, H. *Phys. Rev. B* **2006**, *74*, 094202.
- (16) Messina, F.; Cannas, M. *J. Phys. Chem. C* **2007**, *111*, 6663.
- (17) Edwards, A. H.; Fowler, W. B. *Phys. Rev. B* **1982**, *26*, 6649.
- (18) Bongiorno, A.; Pasquarello, A. *Phys. Rev. Lett.* **2002**, *88*, 125901.
- (19) Bakos, T.; Rashkeev, S. N.; Pantelides, S. T. *Phys. Rev. B* **2004**, *69*, 195206.
- (20) Kajihara, K.; Skuja, L.; Hirano, M.; Hosono, H. *Phys. Rev. Lett.* **2004**, *92*, 015504.
- (21) Griscom, D. L. In *Structure and Bonding in Noncrystalline Solids*; Walrafen, G. E., Revesz, A. G., Eds.; Plenum Press: New York, 1986.
- (22) Evans, B. D. *IEEE Trans. Nucl. Sci.* **1988**, *35*, 1215.
- (23) Griscom, D. L. *J. Ceram. Soc. Jpn.* **1991**, *99*, 899.
- (24) Leclerc, N.; Pfeleiderer, C.; Hitzler, H.; Wolfrum, J.; Greulich, K.-O.; Thomas, S.; Englisch, W. *J. Non-Cryst. Solids* **1992**, *149*, 115.
- (25) Griscom, D. L.; Gingerich, M. E.; J.; Friebele, E. *Phys. Rev. Lett.* **1993**, *71*, 1019.
- (26) Griscom, D. L. *Phys. Rev. B* **2001**, *64*, 174201.
- (27) Borgermans, P.; Brichard, B. *IEEE Trans. Nucl. Sci.* **2002**, *49*, 1439.
- (28) Agnello, S.; Nuccio, L. *Phys. Rev. B* **2006**, *73*, 115203.
- (29) Agnello, S.; Boizot, B. *J. Non-Cryst. Solids* **2003**, *322*, 84.
- (30) Levy, P. W. *J. Phys. Chem. Solids* **1991**, *52*, 319.
- (31) Messina, F.; Cannas, M. *Phys. Rev. B* **2005**, *72*, 195212.
- (32) Heraeus Quarzglas. *Base Materials Catalogue*; Hanau, Germany, 2005.
- (33) Kühn, B. (Heraeus Quarzglas GmbH). Private communication.
- (34) Skuja, L. *J. Non-Cryst. Solids* **1998**, *239*, 16.
- (35) Agnello, S.; Boscaino, R.; Cannas, M.; Gelardi, F. M.; Leone, M. *Phys. Rev. B* **2000**, *61*, 1946.
- (36) Agnello, S.; Boscaino, R.; Cannas, M.; Gelardi, F. M. *Phys. Rev. B* **2001**, *64*, 174423.
- (37) Nishikawa, H. In *Silicon-Based Materials and Devices*; Nalwa, H. S., Ed.; Academic Press: New York, 2001.
- (38) Leone, M.; Agnello, S.; Boscaino, R.; Cannas, M.; Gelardi, F. In *Silicon-Based Materials and Devices*; Nalwa, H. S., Ed.; Academic Press: New York, 2001.
- (39) Atkins, P. W.; Paula, J. D. *Atkins' Physical Chemistry*; Oxford University Press: Oxford, U.K., 2004.
- (40) The solution is written within the assumption that  $[E']_0 > 2[H_2]_0$ ; i.e., the initial concentration of hydrogen is insufficient to completely passivate the defects.
- (41) Buscarino, G.; Agnello, S. *J. Non-Cryst. Solids* **2007**, *353*, 577.
- (42) Waite, T. R. *Phys. Rev.* **1957**, *107*, 463.
- (43) Doremus, R. H., Ed. *Diffusion of Reactive Molecules in Solids and Melts*; John Wiley & Sons: New York, 2002.
- (44) It is worth noting that these considerations do not hold for the case of reaction with  $H_2$ , because the latter is not diffusion-limited.<sup>16</sup> However, this is expected to be an exceptional case for reactions of point defects with mobile species in a solid, generally assumed to be diffusion-limited.<sup>3,15,43</sup>
- (45) Tomozawa, M. In *Silicon-Based Materials and Devices*; Nalwa, H. S., Ed.; Academic Press: New York, 2001.
- (46) Doremus, R. H. *J. Mater. Res.* **1995**, *10*, 2379.
- (47) Alternatively, one could say that the distinction between  $D_{H_2O}$  and  $D_{eff}$  is lost.
- (48) Wolf, A. A.; Friebele, E. J.; Griscom, D. L. *J. Non-Cryst. Solids* **1983**, *56*, 349.
- (49) Cannas, M.; Vaccaro, L.; Boscaino, R. *Nucl. Instrum. Methods, B* **2008**, *266*, 2945.
- (50) Shelby, J. E. *J. Non-Cryst. Solids* **1994**, *179*, 138.
- (51) Davis, K. M.; Agarwal, A.; Tomozawa, M.; Hirao, K. *J. Non-Cryst. Solids* **1996**, *203*, 27.
- (52) Davis, K. M.; Tomozawa, M. *J. Non-Cryst. Solids* **1996**, *201*, 177.
- (53) Oehler, A.; Tomozawa, M. *J. Non-Cryst. Solids* **2004**, *347*, 211.